

Synthesis, characterization, photophysical and DNA photocleavage properties of amphiphilic porphyrins

Jie Zhang^{*a}◇, Mingyu Teng^b and Dan Li^c

^a School of Pharmaceutical and Chemical Engineering, Taizhou University, Taizhou 318000, P. R. China

^b Faculty of Chemistry and Chemical Engineering, Yunnan Normal University, Kunming 650500, P. R. China

^c Department of Scientific Research, Taizhou University, Linhai 317000, P. R. China

Received 26 June 2013

Accepted 30 September 2013

ABSTRACT: A series of amphiphilic porphyrins appended with pyridinium cation and/or polyethylene glycol have been synthesized and fully characterized by ¹H NMR, IR and MALDI-TOF-MS. Their photophysical properties were determined and the singlet oxygen (¹O₂) quantum yields of these compounds are in the range of 0.30–0.61 in CHCl₃ and 0.048–0.18 in Tris buffer. The measured two-photon absorption (TPA) cross-sections σ⁽²⁾ of these porphyrin derivatives are between 110 and 240 GM. These amphiphilic porphyrins show some photocleavage activities (10%–21%) towards the anionic DNA observed at 100 μM.

KEYWORDS: singlet oxygen, two-photon absorption, DNA photocleavage, amphiphilic porphyrins.

INTRODUCTION

Photodynamic therapy (PDT) has recently emerged as an inherently selective cancer treatment modality rendered by precisely targeted photodamage of the cancerous tissues. In PDT, non-toxic photosensitizer preferentially accumulates inside the tumor cells and generates cytotoxic reactive oxygen species (*e.g.* singlet oxygen) only when photo-activated *via* absorption at specific wavelengths [1].

The majority of photosensitizers are tetrapyrroles or porphyrinoids, and these drugs cause cell death by transferring energy to oxygen, producing the highly reactive singlet excited state of molecular oxygen, ¹O₂ [2]. An efficient PDT photosensitizer requires a favorable combination of the following factors: (1) light absorption at wavelengths which penetrate effectively into biological tissue (700–950 nm), (2) a high quantum yield for singlet oxygen generation (Φ_Δ), (3) efficient uptake into the diseased tissues, and (4) localisation in regions of the cell which are vulnerable to singlet oxygen damage

[2a, 2c, 3]. There are also other important requirements such as low dark toxicity and good pharmacokinetics.

Recently, a new approach to photogenerate singlet oxygen (¹O₂) *via* two photon excitation of a sensitizer has been reported [4]. Two photon absorption (TPA) is an optical nonlinear process that involving simultaneous absorption of two photons, in which the energy of a photon is normally unable to induce excitation. It can be accomplished by laser light with λ ≥ 800 nm *via* TPA, therefore allowing much better depth penetration through tissues. Porphyrin-based materials show a strong linear absorption at about 400–500 nm. Thus, its TPA should be around 800–1000 nm [5]. It is widely accepted that the optimum excitation wavelength for PDT agents should be within this range to increase the penetration of tissue and minimize the absorption from water. Therefore, porphyrin-based materials are the prior option in TPA-PDT. However, the problem is that the TPA cross-section of commercial available porphyrin-base materials is very low. Therefore, many efforts have been focused on the development of new porphyrin-based materials with high TPA cross-section σ⁽²⁾ values [6].

In this study, we aim to develop porphyrin-based photosensitizers that possess the above mentioned properties optimized for PDT applications and excite

◇SPP full member in good standing

*Correspondence to: Jie Zhang, email: zhang_jie@tzc.edu.cn, tel: +86 576-8513-7265

via TPA. To accomplish this goal, an amphiphilic porphyrin with an appropriate hydrophobic/hydrophilic balance was designed with the H₂TPP (Scheme 1) or H₂TPEGPP (Scheme 2) and its cationic pyridinium group, respectively, as the hydrophobic and the hydrophilic ends. Herein, we report the synthesis, characterization, photophysical and DNA photocleavage activities of these amphiphilic porphyrin derivatives with pyridinium cations and polyethylene glycol.

EXPERIMENTAL

Materials and methods

The chemicals were purchased from Sigma-Aldrich Company and used as received. Silica gel 60 (0.04–0.063 mm) for column chromatography was purchased from Merck. NMR spectra were recorded on a Bruker Ultrashield 400 Plus NMR spectrometer. High-resolution matrix-assisted laser desorption/ionization time-of-flight (MALDI-TOF) mass spectra were recorded with a Bruker Autoflex MALDI-TOF mass spectrometer. All solution spectroscopic measurements were prepared in spectrophotometric grade CHCl₃ and DMSO (Aldrich) and degassed with freeze-pump-thaw cycles (three times). Electronic absorption spectra in the UV-vis region were recorded with a Varian Cary 100 UV-vis spectrophotometer. The IR spectra (KBr pellets) were recorded with a Nicolet Magna 550 FTIR spectrometer. Steady-state visible fluorescence, PL excitation spectra, singlet oxygen and near-IR (NIR) emission spectra were recorded on a Photon Technology International (PTI) Alphascan spectrofluorimeter and visible decay spectra on a pico-N₂ laser system (PTI Time Master) with $\lambda_{\text{exc}} = 337$ nm. Quantum yields of visible emissions were computed according to the literature method using H₂TPP as the reference standard [7]. The absorbance of the solutions for fluorescence quantum yield measurements was less than 0.02 at the excitation wavelength, so that attenuation of the excitation beam in the sample was small. It was computed by using the expression $\Phi_s = \Phi_r(B_r/B_s)(n_s/n_r)^2(D_s/D_r)$, where the subscripts r and s denote reference standard and the sample solution, respectively, and n, D, and Φ are the refractive index of the solvents, the integrated intensity, and the luminescence quantum yield, respectively. The quantity B was calculated by using $B = 1 - 10^{-A}$, where A is the absorbance at the excitation wavelength. All measurements were performed at ambient temperature (20 ± 2 °C) under atmospheric pressure.

Two-photon absorption measurements

The two-photon-absorption spectra (*i.e.* Z-scan traces) were measured at 800 nm by the open-aperture Z-scan method using 100 fs laser pulses with a peak power

of 276 GW cm⁻² from an optical parametric amplifier operating at a repetition rate of 1 kHz generated from a Ti:sapphire regenerative amplifier system [8]. The laser beam was split into two parts by a beam splitter. One was monitored by a photodiode (D1) as the incident intensity reference, I₀, and the other was detected as the transmitted intensity by another photodiode (D2). After passing through a lens with f = 20 cm, the laser beam was focused and passed through a quartz cell. The position of the sample cell, z, was moved along the direction of the laser beam (z axis) by a computer-controlled translatable table so that the local power density within the sample cell could be changed under the constant incident intensity laser power level. Finally, the transmitted intensity from the sample cell was detected by the photodiode D2. The photodiode D2 was interfaced to a computer for signal acquisition and averaging. Each transmitted intensity datum represents the average of over 100 measurements. Assuming a Gaussian beam profile, the nonlinear absorption coefficient, β , can be obtained by curve-fitting to the observed open-aperture traces, T(z), with Equation 1 [9], where α_0 is the linear absorption coefficient, l is the sample length (the 1 mm quartz cell) and z₀ is the diffraction length of the incident beam. After obtaining the nonlinear absorption coefficient, β , the TPA cross-section, $\sigma^{(2)}$, of the sample molecule (in units of 1 GM = 10⁻⁵⁰ cm⁴.s.photon⁻¹) can be determined by using Equation 2, where N_A is Avogadro's constant, d is the concentration of the sample compound in solution, h is Planck's constant and ν is the frequency of the incident laser beam.

$$T(z) = 1 - \frac{\beta I_0 (1 - e^{-\alpha_0 l})}{2\alpha_0 [1 + z/z_0]^2} \quad (1)$$

$$\sigma^{(2)} = \frac{1000\beta h\nu}{N_A d} \quad (2)$$

DNA photocleavage assay (plasmid DNA relaxation assay)

The DNA photocleavage activities of the test samples were measured using the plasmid DNA relaxation assay. Briefly, the plasmid DNA (pBluescript), enriched with the covalently-closed circular conformer, and the one-phor-all plus buffer (10 mM Tris-acetate, 10 mM magnesium acetate, 50 mM potassium acetate, pH 7.5) was vortexed. Aliquots of the DNA were pipetted into different Eppendorf tubes. Various amounts of autoclaved water (control sample) or test samples were added into the Eppendorf tubes to give a final volume 20 L in each sample tube. The sample mixtures were then photo-irradiated either at 400–500 nm for 30 or 45 min using a transilluminator (Vilber Lourmat) containing 4 × 15 W light tubes (Aqua Lux) with maximum emission at 455 nm or at > 605 nm using a 50 W halogen lamp equipped with an optical filter which cutoff all wavelengths shorter

than 605 nm. After photo-irradiation, 3 μL of the 6X sample dye solution (which contained 20% glycerol, 0.25% bromophenol blue and 0.25% xylene cyanol FF) was added to each Eppendorf tube and mixed well by centrifugation. The sample mixtures were loaded onto a 0.8% (v/v) agarose gel (dimension: 13 cm \times 10 cm), with 1X Tris-borate-EDTA buffer (89 mM Tris-borate, 2.5 mM EDTA, pH 8) used as supporting electrolyte, and electrophoresized at 1.3 V.cm⁻¹ for 3 h using mini gel set (CBS Scientific Co., Model MGU-502T). After electrophoresis, the gel was stained with 0.5 g/mL ethidium bromide solution for 10 min and then destained with deionized water for 3 min. The resulting gel image was viewed under 365 nm light and captured digitally using a gel documentation system (BioRad).

Preparations of porphyrin derivatives with pyridinium cations and polyethylene glycol

***p*-OH-TPP.** A solution of benzaldehyde (18.29 mL, 180 mmol) and *p*-hydroxybenzaldehyde (7.32 g, 60 mmol) in propionic acid (700 mL) was heated to 130 °C. Then freshly distilled pyrrole (16.65 mL, 240 mmol) in propionic acid (50 mL) was added slowly to the solution over a period of 0.5 h. The reaction mixture was heated to reflux for another 0.5 h and then cooled to rt. Then the volume of the reaction mixture was reduced to about half of its original volume under reduced pressure, and methanol (300 mL) was added to the concentrated solution. The resultant solution was kept in a refrigerator overnight to give dark purple solid, which was filtered, redissolved in a minimum amount of CHCl₃ and chromatographed on a silica gel column with CH₂Cl₂ as eluent. The second band gave the desired *p*-OH-TPP. Yield 1.8 g (4.8%). ¹H NMR (400 MHz; CDCl₃; Me₄Si): δ_{H} , ppm 8.86–8.84 (m, 8H), 8.23–8.20 (m, 6H), 8.06 (d, J = 8.4 Hz, 2H), 7.77–7.74 (m, 9H), 7.17 (d, J = 8.8 Hz, 2H), 5.07 (s, 1H) and -2.78 (s, 2H). HRMS (MALDI-TOF, +ve mode, CHCl₃): m/z 630.2455 (calcd. for [M]⁺ 630.2414). IR (KBr): ν , cm⁻¹ 3502w, 3314w, 3053w, 1662m, 1594m, 1472s, 1170m, 965s, 798s and 699s.

TPP-OC₆Br. 1,6-dibromohexane (1.23 mL, 8.0 mmol) was added to a suspension of *p*-OH-TPP (500 mg, 0.80 mmol) and anhydrous K₂CO₃ in dry DMF (20 mL). The mixture was stirred at rt, and the progress of the reaction was monitored by TLC. After 24 h, CH₂Cl₂ (20 mL) was added to the reaction mixture, which was then washed with water (6 \times 20 mL) until all of the DMF and K₂CO₃ were removed. The organic phase was dried with Na₂SO₄, filtered and the solvents were evaporated to dryness under vacuum. The residue was redissolved in a CHCl₃/hexane mixture (1:1, v/v) and chromatographed on a silica gel column using CHCl₃/hexane (5:1, v/v) as eluent. The first band gave the product TPP-OC₆Br. Yield 544 mg (86.3%). ¹H NMR (400 MHz; CDCl₃; Me₄Si): δ_{H} , ppm 8.89–8.88 (m, 8H), 8.22–8.21 (m, 6H), 8.11 (d, J = 8.8 Hz, 2H), 7.78–7.73 (m, 9H), 7.28–7.26 (m, 2H),

4.24 (t, J = 6.4 Hz, 2H), 3.51 (t, J = 6.4 Hz, 2H), 32.02–2.00 (m, 4H), 1.68–1.66 (m, 4H) and -2.77 (s, 2H). HRMS (MALDI-TOF, positive mode, CHCl₃): m/z 794.2469 (calcd. for [M]⁺ 794.2449). IR (KBr): ν , cm⁻¹ 3314m, 3052w, 2927m, 1596m, 1466s, 1245s, 1175s, 965s, 780vs and 701s. UV-vis (CHCl₃, 20 °C): λ_{max} , nm (log ϵ , M⁻¹.cm⁻¹) 418 (5.63), 516 (4.18), 551 (3.81), 591 (3.54) and 647 (3.57).

TPP-OC₆-Py-OH. 4-hydroxyl pyridine (120 mg, 1.26 mmol) was added to a suspension of TPP-OC₆Br (100 mg, 0.13 mmol) and anhydrous K₂CO₃ in dry DMF (10 mL). The mixture was stirred at room temperature, and the progress of the reaction was monitored by TLC. After 24 h, the mixture was evaporated to dryness under vacuum. The residue was redissolved in a CHCl₃ and chromatographed on a silica gel column using CHCl₃/CH₃OH as eluent. The third band gave the product TPP-OC₆-Py-OH. Yield 73 mg (71.8%). ¹H NMR (400 MHz; CDCl₃; Me₄Si): δ_{H} , ppm 8.88–8.87 (m, 8H), 8.85–8.21 (m, 6H), 8.11 (d, J = 8.4 Hz, 2H), 7.78–7.75 (m, 9H), 7.29–7.24 (m, 4H), 6.43 (d, J = 6.4, 2H), 4.22 (t, J = 6.4 Hz, 2H), 3.78 (t, J = 7.2 Hz, 2H), 1.97–1.92 (m, 2H), 1.89–1.82 (m, 2H), 1.66–1.62 (m, 2H), 1.50–1.44 (m, 2H) and -2.78 (s, 2H). HRMS (MALDI-TOF, positive mode, CHCl₃): m/z 808.3604 (calcd. for [M]⁺ 808.9855). IR (KBr): ν , cm⁻¹ 3430m, 3313m, 2934m, 1636m, 1578s, 1468s, 1243s, 1182s, 965s, 799s and 747vs. UV-vis (CHCl₃, 20 °C): λ_{max} , nm (log ϵ , M⁻¹.cm⁻¹) 418 (5.66), 515 (4.27), 551 (4.00), 590 (3.84) and 647 (3.85).

ZnTPP-OC₆Br. The complex was prepared by refluxing TPP-OC₆Br (570 mg, 0.72 mmol) with an excess amount of zinc(II) acetate in CHCl₃/methanol for 5 h; it was then purified by column chromatography on silica gel with CHCl₃ as eluent. Yield 520 mg, 84.6%. ¹H NMR (CDCl₃): δ_{H} , ppm 8.99–8.94 (m, 8H), 8.23–8.21 (m, 6H), 8.10 (d, J = 8.4, 2H), 7.77–7.71 (m, 9H), 7.24–7.23 (m, 2H), 4.21 (m, 2H), 3.49 (t, J = 6.4, 2H), 2.00–1.97 (m, 4H) and 1.65–1.63 (m, 4H). HRMS (MALDI-TOF, positive mode, CHCl₃): m/z 856.1600 (calcd. for [M]⁺ 856.1577). IR (KBr): ν , cm⁻¹ 3434m, 3049m, 2929s, 1596s, 1486s, 1248vs, 1174s, 1003vs, 798vs and 701s. UV-vis (CHCl₃, 20 °C): λ_{max} , nm (log ϵ , M⁻¹.cm⁻¹) 419 (5.78), 547 (4.28) and 585 (3.11).

ZnTPP-OC₆-Py-OH. 4-hydroxyl pyridine (240 mg, 2.53 mmol) was added to a suspension of ZnTPP-OC₆Br (200 mg, 0.23 mmol) and anhydrous K₂CO₃ in dry DMF (10 mL). The mixture was stirred at room temp, and the progress of the reaction was monitored by TLC. After 24 h, the mixture was evaporated to dryness *in vacuo*. The residue was redissolved in a CHCl₃ and chromatographed on a silica gel column using CHCl₃/CH₃OH as eluent. The third band gave the product TPP-OC₆-Py-OH. Yield 120 mg (59.1%). ¹H NMR (400 MHz; CDCl₃; Me₄Si): δ_{H} , ppm 8.84 (m, 8H), 8.83–8.82 (m, 6H), 7.99 (d, J = 8.4 Hz, 2H), 7.72–7.65 (m, 9H), 7.08 (d, J = 8.4 Hz, 2H), 6.28 (d, J = 7.6 Hz, 2H), 4.04 (d, J = 6.8, 2H), 3.91 (t, J = 6.4, 2H), 2.91 (t, J = 6.8, 2H), 1.56 (m, 2H), 1.19–1.14

(m, 4H) and 0.83–0.81 (m, 2H). HRMS (MALDI-TOF, positive mode, CHCl₃): *m/z* 870.2807 (calcd. for [M]⁺ 870.2780). IR (KBr): ν , cm⁻¹ 3434m, 2926m, 1635vs, 1560vs, 1486s, 1247s, 1186s, 992s, 797s and 751s. UV-vis (CHCl₃, 20 °C): λ_{max} , nm (log ϵ , M⁻¹.cm⁻¹) 420 (5.73), 549 (4.24) and 589 (3.23).

***p*-OHTPEGPP.** A solution of 4-[tri(ethylene glycol) monomethyl ether] benzaldehyde (13 g, 0.048 mol) and *p*-hydroxybenzaldehyde (1.97 g, 0.016 mol) in propionic acid (300 mL) was heated to 130 °C. Then freshly distilled pyrrole (4.47 mL, 0.064 mol) in propionic acid (50 mL) was added slowly to the solution over a period of 0.5 h. The reaction mixture was heated to reflux for another 0.5 h and then cooled to rt. Then the volume of the reaction mixture was reduced to about 20 mL under reduced pressure, and ethanol (300 mL) was added to the concentrated solution. The resultant solution was kept in a refrigerator overnight to give purple solid, which was filtered, redissolved in a minimum amount of CHCl₃ and chromatographed on a silica gel column with CH₂Cl₂/CH₃OH as eluent. The first band gave the 5,10,15,20-tetraPEGphenylporphyrin. The second band gave the desired *p*-OHTPEGPP, Yield 600 mg (3.4%). ¹H NMR (400 MHz; CDCl₃; Me₄Si): δ_{H} , ppm 8.83–8.77 (m, 8H), 8.03–7.94 (m, 8H), 7.19–7.11 (m, 8H), 5.70 (s, 1H), 4.34–4.26 (m, 6H), 4.02–3.98 (m, 6H), 3.85–3.72 (m, 18H), 3.61–3.60 (m, 6H), 3.41 (s, 9H) and -2.81 (s, 2H). HRMS (MALDI-TOF, positive mode, CHCl₃): *m/z* 1117.5109 (calcd. for [M + H]⁺ 1117.5168). IR (KBr): ν , cm⁻¹ 3320m, 2923m, 1607s, 1508s, 1472s, 1247s, 1176s, 967s, 805s and 741vs. UV-vis (CHCl₃, 20 °C): λ_{max} , nm (log ϵ , M⁻¹.cm⁻¹) 421 (5.35), 519 (3.50), 553 (3.19) and 651 (3.15).

TPEGPP. Yield 505 mg (2.5%). ¹H NMR (400 MHz; CDCl₃; Me₄Si): δ_{H} , ppm 8.85 (s, 8H), 8.10 (d, *J* = 8.8 Hz, 8H), 7.30–7.25 (m, 8H), 4.43–4.40 (m, 8H), 4.06–4.03 (m, 8H), 3.89–3.87 (m, 8H), 3.80–3.78 (m, 8H), 3.75–3.73 (m, 8H), 3.63–3.61 (m, 8H), 3.42 (s, 12H) and -2.77 (s, 2H). HRMS (MALDI-TOF, positive mode, CHCl₃): *m/z* 1263.6148 (calcd. for [M + H]⁺ 1263.6112). IR (KBr): ν , cm⁻¹ 3320m, 2925s, 1606s, 1502s, 1455s, 1246s, 1177s, 967s, 803s and 741vs. UV-vis (CHCl₃, 20 °C): λ_{max} , nm (log ϵ , M⁻¹.cm⁻¹) 421 (5.51), 519 (3.78), 555 (3.54), 594 (1.27) and 652 (3.33).

TPEGPP-PEG-I. 1-iodo-2-(2-(2-(2-iodoethoxy)ethoxy)ethoxy)ethane (444 mg, 1.074 mmol) was added to a suspension of *p*-OHTPEGPP (60 mg, 0.0537 mmol) and anhydrous K₂CO₃ in DMF (5 mL). The mixture was stirred at room temp, and the progress of the reaction was monitored by TLC. After 24 h, the mixture was evaporated to dryness *in vacuo*. The residue was redissolved in CHCl₃ and chromatographed on a silica gel column using CHCl₃/CH₃OH as eluent. The first band gave the product TPEGPP-PEG-I. Yield 50 mg (66.7%). ¹H NMR (400 MHz; CDCl₃; Me₄Si): δ_{H} , ppm 8.85 (s, 8H), 8.11 (d, *J* = 8.4 Hz, 8H), 7.30–7.29 (m, 8H), 4.44 (m, 8H), 4.07 (m, 8H), 3.89–3.88 (m, 8H), 3.81–3.79 (m, 10H),

3.75–3.74 (m, 10H), 3.64–3.62 (m, 6H), 3.43 (s, 9H), 3.32–3.29 (m, 2H) and -2.78 (s, 2H). HRMS (MALDI-TOF, positive mode, CHCl₃): *m/z* 1403.5291 (calcd. for [M + H]⁺ 1403.5234). IR (KBr): ν , cm⁻¹ 3318m, 2876m, 1607s, 1508s, 1472s, 1247vs, 1176s, 967s, 804s and 740m. UV-vis (CHCl₃, 20 °C): λ_{max} , nm (log ϵ , M⁻¹.cm⁻¹) 421 (5.35), 519 (3.11), 555 (1.86) and 651 (2.37).

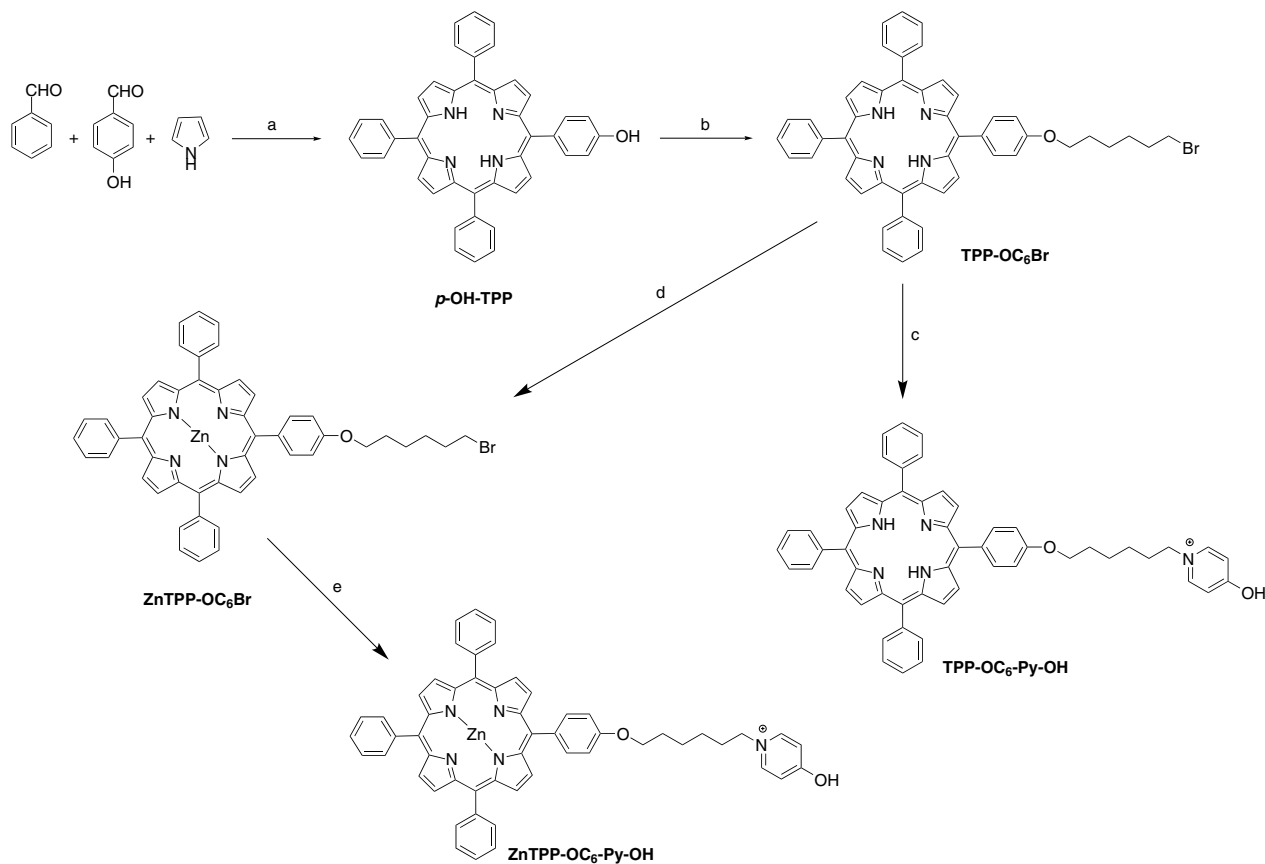
TPEGPP-PEG-Py-OH. 4-hydroxypyridine (21 mg, 2.2 mmol) was added to a suspension of TPEGPP-PEG-I (32 mg, 0.022 mmol) and anhydrous K₂CO₃ in dry DMF (3 mL). The mixture was stirred at 60 °C, and the progress of the reaction was monitored by TLC. After 24 h, the mixture was evaporated to dryness *in vacuo*. The residue was redissolved in a CHCl₃ and chromatographed on a silica gel column using CHCl₃/CH₃OH as eluent. The third band gave the product TPEGPP-PEG-Py-OH. Yield 17 mg (54.8%). ¹H NMR (400 MHz; CDCl₃; Me₄Si): δ_{H} , ppm 8.90 (s, 8H), 8.10 (d, *J* = 8.4 Hz, 8H), 7.33–7.26 (m, 10H), 6.37 (d, *J* = 7.6, 2H), 4.43–4.40 (m, 8H), 4.06–4.04 (m, 8H), 3.88–3.79 (m, 16H), 3.74 (m, 10H), 3.63–3.62 (m, 10H), 3.42 (s, 9H) and -2.72 (s, 2H). HRMS (MALDI-TOF, positive mode, CHCl₃): *m/z* 1370.6454 (calcd. for [M]⁺ 1370.6488). IR (KBr): ν , cm⁻¹ 3316m, 2922m, 1639s, 1503s, 1454s, 1246vs, 1176s, 966s, 803s and 741m. UV-vis (CHCl₃, 20 °C): λ_{max} , nm (log ϵ , M⁻¹.cm⁻¹) 421 (5.28), 518 (3.55), 555 (3.33), 591 (2.56) and 650 (2.88).

RESULT AND DISCUSSION

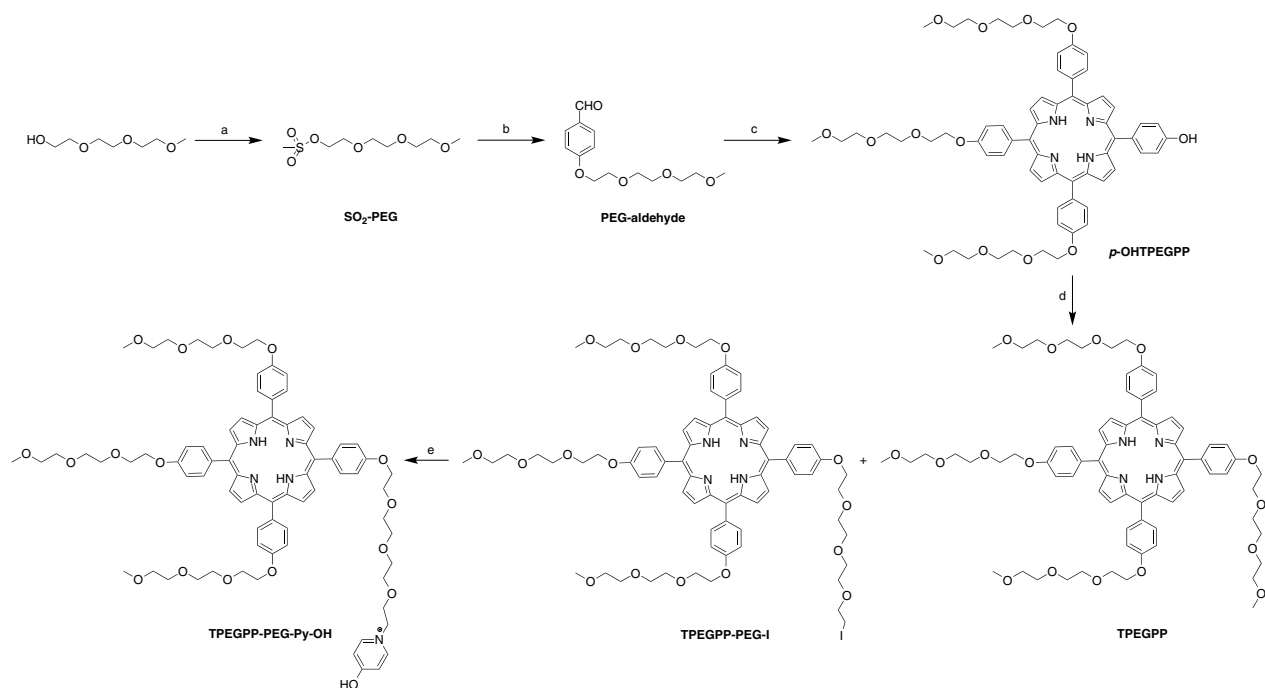
Synthesis of amphiphilic porphyrins

The synthetic routes for amphiphilic porphyrins TPP-OC₆-Py-OH and ZnTPP-OC₆-Py-OH are shown in Scheme 1. Carbon chain was attached to *p*-OHTPPH₂ by nucleophilic substitution reaction between phenol group of the porphyrin and bromo-group of 1,6-dibromohexane in the presence of a base (K₂CO₃) using DMF as the solvent. The product TPP-OC₆Br could be easily purified by column chromatography using a silica gel column and the yield was about 86%. TPP-OC₆Br was then further reacted with 4-hydroxyl pyridine in DMF to give TPP-OC₆-Py-OH in about 72% yield. Reaction of TPP-OC₆Br with an excess amount of zinc(II) acetate in CHCl₃/methanol give the product ZnTPP-OC₆Br in about 85% yield. ZnTPP-OC₆Br was then further reacted with 4-hydroxyl pyridine in DMF to give ZnTPP-OC₆-Py-OH in about 59% yield. The advantage of this synthetic route is that the carbon length can be adjusted.

The synthetic routes for the preparation of amphiphilic porphyrin TPEGPP-PEG-Py-OH are shown in Scheme 2. Reaction of polyethylene glycol (PEGOH) with methanesulfonyl chloride gave the product SO₂-PEG in good yield. Polyethylene glycol substituted aldehyde was synthesized by a nucleophilic reaction between 4-hydroxybenzaldehyde and SO₂-PEG. Then, polyethylene glycol



Scheme 1. Synthetic route for ZnTPP-OC₆-Py-OH. (a) propionic acid, reflux. (b) 1,6-dibromohexane, K₂CO₃, DMF, rt. (c) 4-hydroxyl pyridine, DMF, rt. (d) zinc(II) acetate, CHCl₃/methanol, reflux. (e) 4-hydroxyl pyridine, DMF, rt



Scheme 2. Synthetic routes for TPEGPP-PEG-Py-OH. (a) sulfonyl chloride, diisopropylethylamine, 0 °C, (b) 3-hydroxybenzaldehyde, K₂CO₃, THF, 70 °C, (c) 4-hydroxybenzaldehyde, pyrrole, propionic acid, reflux, (d) 1-iodo-2-(2-(2-(2-iodoethoxy) ethoxy) ethoxy) ethane, K₂CO₃, DMF, rt, and (e) 4-Hydroxyl pyridine, DMF, 60 °C

substituted aldehyde and *p*-hydroxybenzaldehyde was refluxed in propionic acid to give the products *p*-OHTPEGPP (3.4%) and TPEGPP (2.5%). PEG-I chain was attached to *p*-OHTPEGPP and TPEGPP-PEG-I could be easily purified by column chromatography with the yield of 67%. TPEGPP-PEG-I was then further reacted with 4-hydroxyl pyridine in DMF to give the target product (TPEGPP-PEG-Py-OH) in about 55% yield.

Absorptions and emissions of amphiphilic porphyrins

The UV-visible absorptions of these amphiphilic porphyrins retain the characteristics features of H₂TPP and ZnTPP [10]. For example, TPP-OC₆-Py-OH shows a strong Soret band at 418 nm and four Q-bands at 515, 551, 590 and 647 nm. In contrast, Zn(II) complex ZnTPP-OC₆-Py-OH exhibits a similar Soret band at 420 nm and two Q-bands at 549 and 589 nm. The absorption spectra and data of these porphyrins are shown in Fig. 1 and summarized in experimental part, respectively. The fluorescence spectra of these amphiphilic porphyrins also retain the characteristics features of H₂TPP and ZnTPP [10]. The metal-free products emitted at about 650 and 720 nm, whereas the zinc containing products at about 600 and 650 nm. When monitoring the emission wavelength at 650 nm, the excitation spectrum exhibits an intense excitation band around 420 nm, which corresponds to the ground-state absorption spectrum. In any case, the visible emissions in the range of 597–727 nm of all of the porphyrins show quite fast decay time (*i.e.* shorter than 1 μs). The fluorescence quantum yields of these porphyrins are in the range of 0.029–0.13. In Tris buffer, a decrease in quantum yields of fluorescence emission is depicted for all the amphiphilic porphyrins (Table 1). The fluorescence spectra these amphiphilic porphyrins are shown in Fig. 2, and the photophysical

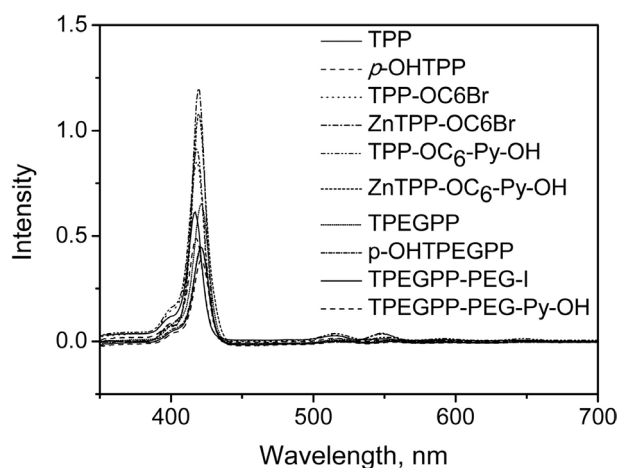


Fig. 1. Absorption spectra of the products in CHCl₃ (2×10^{-6} M)

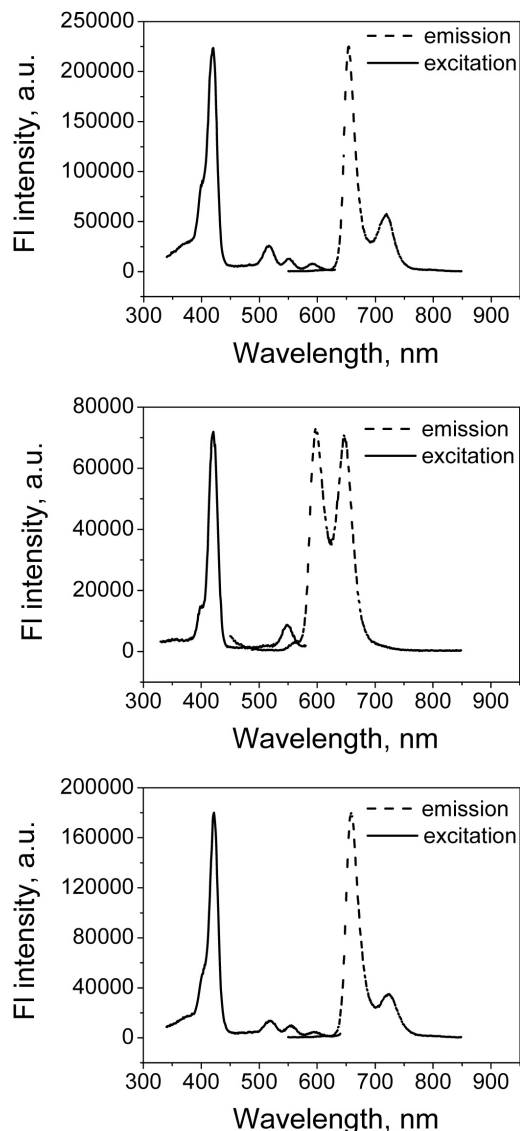


Fig. 2. Excitation and emission spectra of TPP-O-C₆-Py-OH (top) and ZnTPP-O-C₆-Py-OH (middle) and TPEGPP-PEG-Py-OH (bottom) in CHCl₃ (2×10^{-6} M)

data are summarized in Table 1. The results show that the addition of pyridinium and polyethylene glycol moiety has only slight effect on both the absorption and emission of the porphyrin moiety [11].

DNA binding constant experiments

We carried out the EB (ethidium bromide) competitive binding with DNA experiments and the fluorescence quenching plot are given in Fig. 3 [11b]. I_0 and I are the fluorescence intensities in the absence and presence of the porphyrins, respectively. The I_0/I vs. [Por]/[DNA] plot is in good agreement with the linear Stern–Volmer equation with a slope of 0.69, 1.00, 2.40 and 5.09 for TPP-OC₆-Py-OH, ZnTPP-OC₆-Py-OH, *p*-OHTPEGPP and TPEGPP-PEG-Py-OH, respectively. We can also

Table 1. Summary of fluorescence data in CHCl_3 (2×10^{-6} M)

Compound	Excitation, nm	Emission, nm	Φ_f^a	τ_f^c
TPP-OC ₆ Br	420, 516, 550, 591	654, 720	0.094	14.96 ns
ZnTPP-OC ₆ Br	420, 549	597, 648	0.029	1.99 ns
TPP-OC ₆ -Py-OH	420, 516, 551, 591	654, 719	0.096 (0.019) ^b	4.14 ns
ZnTPP-OC ₆ -Py-OH	421, 549	597, 646	0.037 (0.008) ^b	2.13 ns
TPEGPP	422, 518, 555, 593	658, 723	0.130	3.81 ns
<i>p</i> -OHTPEGPP	422, 523, 554, 594	657, 724	0.098 (0.012) ^b	10.07 ns
TPEGPP-PEG-I	422, 520, 556, 594	659, 723	0.096	9.32 ns
TPEGPP-PEG-Py-OH	422, 520, 556, 595	658, 724	0.098 (0.020) ^b	10.61 ns

^aThe fluorescence quantum yields Φ_f were estimated in the benzene, using the integrated emission intensity of 5,10,15,20-tetraphenyl porphyrin (H_2TPP , $\Phi_f = 0.11$ in benzene) as reference [7] (under identical photoirradiation conditions ($\lambda_{\text{exc}} = 420$ nm, $\text{abs}(\lambda_{\text{exc}}) = 0.02$)). ^bThe fluorescence quantum yields Φ_f were estimated in the Tris buffer. ^cThe fluorescence life is measured at excited wavelength = 337 nm in benzene.

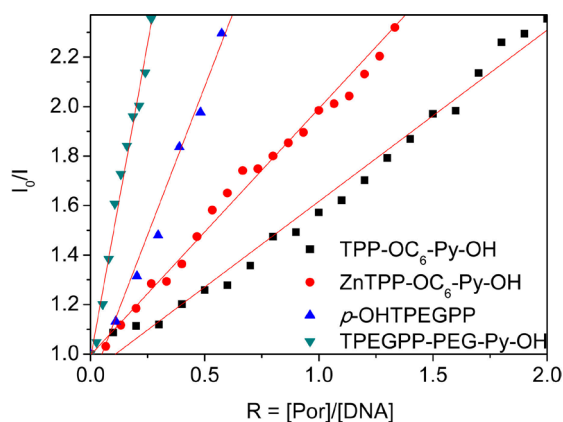


Fig. 3. Fluorescence quenching curves of DNA-bound EB by amphiphilic porphyrins in Tris buffer (pH = 7.2, 0.05 M NaCl) ([DNA] = 100 μM , [EB] = 16.0 μM , $\lambda_{\text{exc}} = 537$ nm)

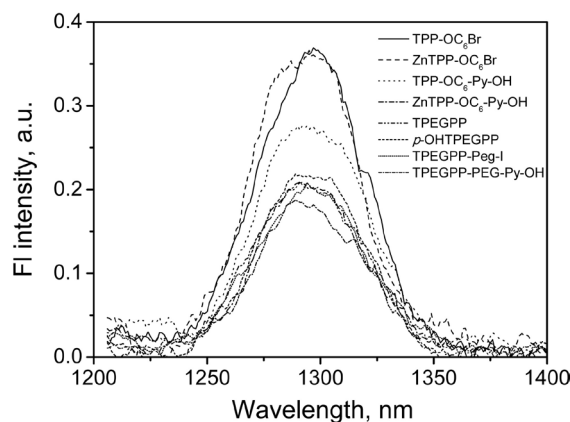


Fig. 4. Near-IR phosphorescence spectra of singlet oxygen $^1\text{O}_2$ produced from the products in CHCl_3 under identical photoirradiation conditions ($\lambda_{\text{exc}} = 420$ nm, $\text{abs}(\lambda_{\text{exc}}) = 0.02$)

learn from Fig. 3 that 50% of EB molecules were replaced from DNA-bound EB at a concentration ratio of $[\text{Por}]/[\text{EB}] = 9.7, 6.3, 2.9$ and 1.3 for TPP-OC₆-Py-OH, ZnTPP-OC₆-Py-OH, *p*-OHTPEGPP and TPEGPP-PEG-Py-OH, respectively. The K_{app} of EB in the experimental condition is $1.0 \times 10^7 \text{ M}^{-1}$ [12], therefore, the K_{app} of TPP-OC₆-Py-OH, ZnTPP-OC₆-Py-OH, *p*-OHTPEGPP and TPEGPP-PEG-Py-OH were $1.03 \times 10^6 \text{ M}^{-1}$ and $1.59 \times 10^6 \text{ M}^{-1}$, $3.49 \times 10^6 \text{ M}^{-1}$ and $7.69 \times 10^6 \text{ M}^{-1}$, respectively [13].

Determination of singlet oxygen ($^1\text{O}_2$) quantum yield

The production of singlet oxygen ($^1\text{O}_2$) can be measured by its phosphorescence at 1270 nm and its quantum yield can be determined by comparing with H_2TPP ($\Phi_{\Delta} = 0.55$). Figure 4 shows the phosphorescence spectra of singlet oxygen ($^1\text{O}_2$) generated

Table 2. Summary of singlet oxygen quantum yields

Compound	Φ_{Δ}^a	Φ_{Δ}^b
TPP-OC ₆ Br	0.61	
ZnTPP-OC ₆ Br	0.53	
TPP-OC ₆ -Py-OH	0.46	0.064
ZnTPP-OC ₆ -Py-OH	0.36	0.048
TPEGPP	0.36	
<i>p</i> -OHTPEGPP	0.33	0.18
TPEGPP-PEG-I	0.33	
TPEGPP-PEG-Py-OH	0.30	0.094

^aThe singlet oxygen quantum yields of these compounds were measured in CHCl_3 relative to H_2TPP ($\Phi_{\Delta} = 0.55$). The experimental uncertainty was *ca.* 20%. ^bSinglet oxygen quantum yields estimated in Tris buffer.

by the photo-irradiation of the samples in CHCl_3 . In general, the singlet oxygen ($^1\text{O}_2$) quantum yields of these porphyrins without polyethylene glycol moiety are slightly greater than those with polyethylene glycol moiety in CHCl_3 . However, a decrease in singlet oxygen ($^1\text{O}_2$) quantum yields (0.048–0.18) for all the amphiphilic porphyrins in Tris buffer (Table 2). Among them, *p*-OHTPEGPP and TPEGPP-PEG-Py-OH showed better result, which indicates nonpegylated porphyrins much more tend to be aggregated in buffer solutions [14]. The relative good singlet oxygen ($^1\text{O}_2$) quantum yields indicate these amphiphilic porphyrins can be applied in PDT application.

Two photon absorption of these porphyrins

The TPA cross-sections $\sigma^{(2)}$ of these porphyrins were measured at 800 nm using 100 fs laser pulses with the open-aperture Z-scan method. Figure 5 shows the representative Z-scan traces of these compounds, from which the absolute $\sigma^{(2)}$ values can be evaluated (Table 3). These porphyrins with different substitutions exhibit slightly different $\sigma^{(2)}$ values between 110 and 240 GM. Although the exceptionally large $\sigma^{(2)}$ values more than 11000 GM on porphyrin derivatives has been reported by Anderson *et al.* [5b], the $\sigma^{(2)}$ values of up to 240 GM are still high among previous reported porphyrin derivatives to date. Therefore, these porphyrins have the potential to produce singlet oxygen ($^1\text{O}_2$) *via* two photon excitation, which is extremely important in the photodynamic therapy (PDT).

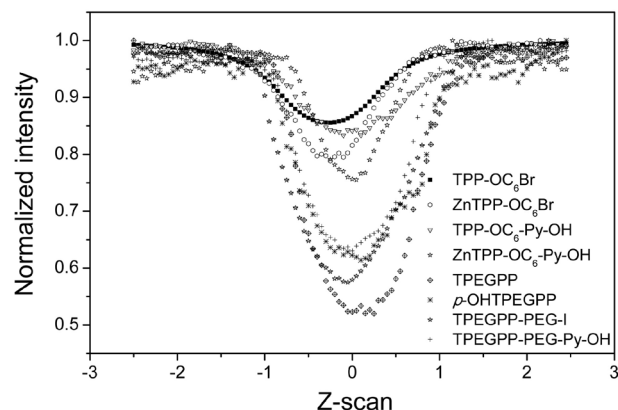


Fig. 5. Open-aperture Z-scan traces of products excited at 800 nm in DMSO (1×10^{-3} M)

Table 3. Summary of TPA cross-section ($\sigma^{(2)}$) data in DMSO (1×10^{-3} M)

Compound	$\sigma^{(2)}$ [GM]	Compound	$\sigma^{(2)}$ [GM]
TPP-OC ₆ Br	110	TPEGPP	198
ZnTPP-OC ₆ Br	171	<i>p</i> -OHTPEGPP	189
TPP-OC ₆ -Py-OH	132	TPEGPP-PEG-I	240
ZnTPP-OC ₆ -Py-OH	170	TPEGPP-PEG-Py-OH	214

DNA photocleavage assay

The DNA photocleavage activities of these amphiphilic porphyrins, namely, ZnTPP-OC₆-Py-OH, TPP-OC₆-Py-OH, *p*-OHTPEGPP and TPEGPP-PEG-Py-OH,

Table 4. Agarose gel image of DNA photocleavage assay of amphiphilic porphyrins in 20% glycerol as a function of its concentration. Lane 1: supercoiled DNA (Form I) alone (control); lane 2: 10 μM amphiphilic porphyrins; lane 3: 20 μM amphiphilic porphyrins; lane 4: 100 μM amphiphilic porphyrins. Photo-irradiation conditions: $\lambda_{\text{irrad}} = 455$ nm; duration 45 min

Conc., μM	0	10	20	100	Conc., μM	0	10	20	100
ZnTPP-OC ₆ -Py-OH					TPP-OC ₆ -Py-OH				
Form II	2	4	6	12	Form II	2	3	4	4
Form I	98	96	94	88	Form I	98	97	96	96
Cleavage activity	0	2	4	10	Cleavage activity	0	1	2	2
Conc., μM	0	10	20	100	Conc., μM	0	10	20	100
<i>p</i> -OHTPEGPP					TPEGPP-PEG-Py-OH				
Form II	2	4	8	23	Form II	2	4	4	4
Form I	98	96	92	77	Form I	98	96	96	96
Cleavage activity	0	2	6	21	Cleavage activity	0	2	2	2

were also measured. Among them, Only ZnTPP-OC₆-Py-OH and *p*-OHTPEGPP showed some photocleavage activities towards the anionic DNA, with 10% and 21% cleavage activities observed at 100 μM, respectively (Table 4). As for *p*-OHTPEGPP, its relatively significant DNA photocleavage activities are likely the result of the highest singlet oxygen (¹O₂) quantum yields and large binding constant with DNA. This result underscores the importance of good singlet oxygen (¹O₂) quantum yields and a close range interaction with the target in effecting the desired outcome [15].

Furthermore, photodynamic therapy (PDT) properties of these products are in testing.

CONCLUSION

In conclusion, a series of amphiphilic porphyrins with pyridinium cations and/or polyethylene glycol, namely, ZnTPP-OC₆-Py-OH, TPP-OC₆-Py-OH, *p*-OHTPEGPP and TPEGPP-PEG-Py-OH, were synthesized and fully characterized by ¹H NMR, IR and MALDI-TOF-MS. Their photophysical properties were investigated in detail. These porphyrin derivatives show good singlet oxygen (¹O₂) quantum yield and exhibit large TPA cross-sections σ⁽²⁾ values between 110 and 240 GM, which indicate they are good candidate as photosensitizers in the PDT applications. In addition, ZnTPP-OC₆-Py-OH and *p*-OHTPEGPP show moderate photocleavage activities (10–21%) towards the anionic DNA observed at 100 μM.

Acknowledgements

This work was supported by the Zhejiang Provincial Natural Science Foundation of China (Grant No. LQ13B010001) and Scientific Research Foundation of Taizhou University (Grant No. 2013PY28).

REFERENCES

1. a) Peng Q, Dougherty TJ, Gomer CJ, Henderson BW, Jori G, Kessel D, Korbelik M and Moan J. *J. Natl. Cancer Inst.* 1998; **90**: 889–905. b) Sakamoto FH, Torezan L and Anderson RR. *J. Am. Acad. Dermatol.* 2010; **63**: 195–211. c) Celli JP, Spring BQ, Rizvi I, Evans CL, Samkoe KS, Verma S, Pogue BW and Hasan T. *Chem. Rev.* 2010; **110**: 2795–2838. d) Robertson CA, Evans DH and Abrahamse H. *J. Photochem. Photobiol. B* 2009; **96**: 1–8.
2. a) Ethirajan M, Chen YH, Joshi P and Pandey RK. *Chem. Soc. Rev.* 2011; **40**: 340–362. b) Daicovicu D, Filip A, Ion RM, Clichici S, Decea N and Muresan A. *Folia. Biol. (Praha)* 2011; **57**: 12–19. c) Chen JX, Wang HY, Li C, Han K, Zhang XZ and Zhuo RX. *Biomaterials* 2011; **32**: 1678–1684. d) Achelle S, Couleaud P, Baldeck P, Teulade-Fichou MP and Maillard P. *Eur. J. Org. Chem.* 2011: 1271–1279.
3. a) Zaruba K, Kralova J, Rezanka P, Pouckova P, Veverkova L and Kral V. *Org. Biomol. Chem.* 2010; **8**: 3202–3206. b) Rani-Beeram S, Meyer K, McCrate A, Hong YL, Nielsen M and Swavey S. *Inorg. Chem.* 2008; **47**: 11278–11283.
4. a) Ogilby PR, Frederiksen PK and Jorgensen M. *J. Am. Chem. Soc.* 2001; **123**: 1215–1221. b) Garcia G, Hammerer F, Poyer F, Achelle S, Teulade-Fichou MP and Maillard P. *Biorg. Med. Chem.* 2013; **21**: 153–165. c) Qian J, Wang D, Cai FH, Zhan QQ, Wang YL and He SL. *Biomaterials* 2012; **33**: 4851–4860. d) Gao L, Fei JB, Zhao J, Li H, Cui Y and Li JB. *Acc Nano* 2012; **6**: 8030–8040. e) Zhao YX, Wang WJ, Wu FP, Zhou Y, Huang NY, Gu Y, Zou QL and Yang W. *Org. Biomol. Chem.* 2011; **9**: 4168–4175.
5. a) Nowak-Krol A, Wilson CJ, Drobizhev M, Kondratuk DV, Rebane A, Anderson HL and Gryko DT. *Chemphyschem.* 2012; **13**: 3966–3972. b) Odom SA, Webster S, Padilha LA, Peceli D, Hu H, Nootz G, Chung SJ, Ohira S, Matichak JD, Przhonska OV, Kachkovski AD, Barlow S, Bredas JL, Anderson HL, Hagan DJ, Van Stryland EW and Marder SR. *J. Am. Chem. Soc.* 2009; **131**: 7510–7511. c) Thorley KJ, Hales JM, Anderson HL and Perry JW. *Angew. Chem. Int. Edit.* 2008; **47**: 7095–7098.
6. a) Pawlicki M, Collins HA, Denning RG and Anderson HL. *Angew. Chem. Int. Edit.* 2009; **48**: 3244–3266. b) Garcia G, Hammerer F, Poyer F, Achelle S, Teulade-Fichou MP and Maillard P. *Biorg. Med. Chem.* 2013; **21**: 153–165.
7. Seybold PG and Gouterman M. *J. Mol. Spectrosc.* 1969; **31**: 1–13.
8. a) Sheik-Bahae M, Said AA, Wei TH, Hagan DJ and Van Stryland EW. *IEEE J. Quantum Electron.* 1990; **26**: 760–769. b) Zhao W and Palffy-Muhoray P. *Appl. Phys. Lett.* 1994; **65**: 673–675.
9. Lee N, Chan PKS, Wong CK, Wong KT, Choi KW, Joynt GM, Lam P, Chan MCW, Wong BCK, Lui GCY, Sin WWY, Wong RYK, Lam WY, Yeung ACM, Leung TF, So HY, Yu AWY, Sung JJY and Hui DSC. *Antivir. Ther.* 2011; **16**: 237–247.
10. a) Kim JB, Leonard JJ and Longo FR. *J. Am. Chem. Soc.* 1972; **94**: 3986–3992. b) Harriman A. *J. Chem.*
- e) Li DH, Diao JL, Wang D, Liu JC and Zhang JT. *J. Porphyrins Phthalocyanines* 2010; **14**: 547–555.
- f) Rodriguez L, de Bruijn HS, Di Venosa G, Mamone L, Robinson DJ, Juarranz A, Batlle A and Casas A. *J. Photochem. Photobiol. B* 2009; **96**: 249–254.
- g) Davia K, King D, Hong YL and Swavey S. *Inorg. Chem. Commun.* 2008; **11**: 584–586.
- h) Mathai S, Smith TA and Ghiggino KP. *Photochem. Photobiol. Sci.* 2007; **6**: 995–1002.
- i) Di Venosa G, Fukuda H, Batlle A, MacRobert A and Casas A. *J. Photochem. Photobiol. B* 2006; **83**: 129–136.
- j) van der Haas RNS, de Jong RLP, Noushazar M, Erkelens K, Smijs TGM, Liu Y, Gast P, Schuitmaker HJ and Lugtenburg J. *Eur. J. Org. Chem.* 2004: 4024–4038.

- Soc., Faraday Trans. 1* 1980; **76**: 1978–1985.
c) Harriman A, Porter G and Searle N. *J. Chem. Soc., Faraday Trans. 2* 1979; **75**: 1515–1521.
11. a) Nawalany K, Kozik B, Kepczynski M, Zapotoczny S, Kumorek M, Nowakowska M and Jachimska B. *J. Phys. Chem. B* 2008; **112**: 12231–12239.
b) Zhao P, Xu LC, Huang JW, Zheng KC, Liu J, Yu HC and Ji LN. *Biophys. Chem.* 2008; **134**: 72–83.
12. Fang YY, Ray BD, Caussen CA, Lipkowitz KB and Long EC. *J. Am. Chem. Soc.* 2004; **126**: 5403–5412.
13. a) Han MJ, Gao LH, Lu YY and Wang KZ. *J. Phys. Chem. B* 2006; **110**: 2364–2371. b) Kumar D, Mishra BA, Shekar KPC, Kumar A, Akamatsu K, Kurihara R and Ito T. *Org. Biomol. Chem.* 2013; **11**: 6675–6679.
14. a) Monteiro CJP, Pereira MM, Azenha ME, Burrows HD, Serpa C, Arnaut LG, Tapia MJ, Sarakha M, Wong-Wah-Chung P and Navaratnam S. *Photochem. Photobiol. Sci.* 2005; **4**: 617–624. b) Nawalany K, Kozik B, Kepczynski M, Zapotoczny S, Kumorek M, Nowakowska M and Jachimska B. *J. Phys. Chem. B* 2008; **112**: 12231–12239. c) Kuimova MK, Collins HA, Balaz M, Dahlstedt E, Levitt JA, Sargent N, Suhling K, Drobizhev M, Makarov NS, Rebane A, Anderson HL and Phillips D. *Org. Biomol. Chem.* 2009; **7**: 889–896.
15. Lu JZ, Pan WJ, He RW, Jin SQ, Liao XW, Wu B, Zhao P and Guo HW. *Transition Met. Chem.* 2012; **37**: 497–503.